


# MULTIDISCIPLINARY DESIGN OF COMPLIANT DEFORMABLE WINGS FOR IMPROVED AIRCRAFT EFFICIENCY: INTRODUCING AN ARCHITECTURE-AWARE OPTIMIZATION STRATEGY

Bradley Blaxall[1], Francesco Di Fiore[1], Demetrios Venetsanos[1] & Laura Mainini[1]

[1]Imperial College London, London, United Kingdom

## Abstract

Trailing-edge morphing airfoils can improve aerodynamic efficiency by adapting camber without the geometric discontinuities of conventional control surfaces. Their design remains inherently multidisciplinary, because the aerodynamic target shape and the compliant mechanism that realizes it under load are strongly coupled. Sequential optimization improves computational tractability by separating aerodynamic target selection from structural realization, but may select geometries whose aerodynamic benefit is lost after structural realization. Coupled optimization evaluates the realized geometry directly, but requires an expensive full aero-structural analysis for every candidate. This paper introduces an architecture-aware Bayesian optimization strategy in which the evaluation architecture is selected during the search rather than fixed a priori. The coupled objective, evaluated on the realized geometry, is retained as the physically relevant design criterion. Lower-cost sequential-type evaluations are used to explore candidate designs through target aerodynamic performance and loaded structural realization, while coupled evaluations are used to assess the aerodynamic response of the realized shape. The approach is demonstrated on a trailing-edge morphing airfoil with an internal compliant beam-network mechanism and compared with standard Bayesian optimization applied to sequential and coupled formulations. Over ten independent runs, architecture-aware Bayesian optimization improves the median realized lift-to-drag ratio by about $10\%$ relative to sequential Bayesian optimization, remains within about $3\%$ of coupled Bayesian optimization, and reduces the median cost at the best design by about $51\%$ relative to the coupled search.

**Keywords:** Multidisciplinary design optimization, architecture-aware Bayesian optimization, morphing wings, camber morphing, compliant structures.

## 1. Introduction

Morphing wing technologies have attracted sustained interest as a means to improve aerodynamic efficiency beyond the limits of fixed-geometry aircraft components [1]. By adapting the external aerodynamic shape during flight, a morphing wing can better accommodate changes in operating condition and mission segment. This capability is particularly relevant in the context of sustainable aviation, where improvements in aerodynamic and structural efficiency are required to support reductions in fuel consumption and greenhouse gas emissions while air-transport demand continues to grow [2, 3]. Among the different morphing concepts investigated in the literature, including span extension [4], sweep variation [5], twist control [6], and camber adaptation [7], trailing-edge camber morphing is especially attractive because it modifies lift and drag characteristics without introducing the sharp geometric discontinuities associated with hinged control surfaces [8, 9].

The practical realization of morphing systems remains a demanding design problem. Mechanisms based on discrete joints, linkages, or smart-material actuation can increase mass, mechanical complexity, and sensitivity to fatigue or reliability issues under repeated operation [10, 11, 12]. These

challenges are amplified in thin trailing-edge regions, where the available internal volume is limited and the external surface must remain sufficiently smooth to preserve aerodynamic performance [13]. Compliant morphing mechanisms offer a possible route to address these limitations by producing shape change through distributed structural flexibility rather than through conventional kinematic joints [14]. For camber-morphing applications, this is attractive because compliance can provide smooth deformation, compact integration, and reduced mechanical discontinuity within the airfoil section [15].

The design of a compliant trailing-edge morphing device is inherently multidisciplinary. The aerodynamic variables define a target shape that is desirable from the standpoint of lift and drag, while the structural variables define the internal mechanism that must reproduce that shape under aerodynamic and actuation loads. These two tasks cannot be separated without consequences. A target airfoil may be aerodynamically efficient but difficult to realize with the available compliant mechanism, may require excessive actuation effort, or may lead to stress, buckling, clearance, or thickness violations.

Multidisciplinary design optimization provides the natural framework for this class of problems because it allows the aerodynamic and structural disciplines to be coordinated within an integrated design optimization process [16, 17, 18]. Existing morphing-wing design studies have addressed this coordination using different optimization architectures. Sequential approaches decompose the problem into disciplinary stages: the aerodynamic problem is solved first to identify target geometries, and the structural problem is then solved to synthesize a mechanism capable of reproducing the selected target [19, 20, 21]. These formulations are computationally convenient because they reduce the dimensionality of each optimization stage, but the aerodynamic target is chosen before the structural realization is fully assessed. Coupled formulations follow a different strategy: the aerodynamic and structural variables are optimized simultaneously, and each candidate is evaluated through a complete aero-structural analysis. This allows the optimizer to account for the interaction between target shape, structural deformation, actuation, and feasibility during the search [22, 23, 24]. These approaches provide a more physically consistent representation of the design problem, but each function evaluation is more expensive and the combined design space is more difficult to explore.

The distinction between sequential and coupled formulations is therefore not only a matter of implementation. It changes what the optimizer is allowed to learn during the search. In a sequential formulation, the optimizer can efficiently expose promising aerodynamic targets, but it may overestimate their final value if the compliant mechanism cannot reproduce them under load. In a coupled formulation, the optimizer evaluates the realized geometry directly, but the cost of doing so for every candidate can severely limit the number of designs explored. For compliant morphing systems, this trade-off is central because the final aerodynamic performance is not determined by the target geometry alone, but by the geometry actually produced by the loaded mechanism.

This paper introduces an architecture-aware Bayesian optimization strategy for the multidisciplinary design optimization of a trailing-edge morphing airfoil. The proposed method treats the evaluation architecture as part of the optimization process: instead of fixing the architecture to be either sequential or fully coupled, the optimizer can choose between a lower-cost sequential-type evaluation and a full coupled evaluation. The method uses Gaussian process regression to approximate two quantities defined over the complete aero-structural design space: (1) the sequential-type objective and (2) the discrepancy between sequential-type and coupled evaluations. The sequential-type objective evaluates the target aerodynamic performance and the loaded structural realization, but it does not recompute the aerodynamics on the realized geometry. The discrepancy accounts for the difference between this lower-cost approximation and the coupled objective evaluated on the geometry actually produced by the compliant mechanism. The acquisition function uses the prediction and associated uncertainty of surrogate model, and the relative evaluation cost to decide which evaluation chain should be queried next. The resulting learning strategy aims to use sequential-type evaluations to explore promising aero-structural candidates at lower cost, while assigning coupled evaluations to designs where capturing the realized aerodynamic benefits is needed to better inform the search.

The architecture-aware Bayesian optimization method is demonstrated on a trailing-edge morphing airfoil equipped with an internal compliant beam-network mechanism. The aerodynamic design

variables parameterize the target camber deformation of the aft airfoil region, while the structural variables define the mechanism geometry, connectivity, sizing, and actuation required to reproduce the target under aerodynamic loading. This setting provides a representative test case for the architecture-aware search because the target aerodynamic performance, loaded shape recovery, actuation effort, and structural feasibility are all coupled through the realized geometry.
The remainder of this manuscript is organized as follows. Section 2. introduces the morphing-airfoil design problem, the sequential and coupled optimization formulations, and the aerodynamic and structural models used to evaluate candidate designs. Section 3. presents the architecture-aware Bayesian optimization strategy, including the surrogate model and acquisition function formulations. Section 4. discusses the experimental results and compares the proposed method with the sequential and coupled standard Bayesian optimization baselines. Section 5. draws concluding remarks.

## 2. Multidisciplinary Design of Trailing-Edge Morphing Airfoil: Problem Setup

The multidisciplinary design problem considered in this work concerns a trailing-edge morphing airfoil equipped with an internal compliant mechanism. The aerodynamic design variables define the target morphed airfoil, whereas the structural design variables define the compliant mechanism used to reproduce that target under aerodynamic loading.
This multidisciplinary problem can be addressed through either a sequential or a coupled optimization strategy. In the sequential architecture, the design task is decomposed into two consecutive subproblems. The aerodynamic optimizer first searches for a target morphed airfoil using aerodynamic performance indicators only. Once the aerodynamic target has been selected, the structural optimizer searches for a compliant mechanism capable of reproducing that target under the prescribed aerodynamic loading, while satisfying stress, buckling, clearance, and actuation constraints. This architecture reflects a discipline-by-discipline design process, in which the aerodynamic target is fixed before structural feasibility is assessed.
In the coupled architecture, the aerodynamic and structural variables are instead optimized simultaneously. Each candidate design is evaluated through the complete aero-structural chain, so that aerodynamic performance, shape recovery, actuation effort, mass, and structural feasibility are assessed within a single design loop. This formulation allows the optimizer to account directly for the interaction between the target aerodynamic shape and the structural mechanism required to realize it. As a result, the coupled problem can avoid aerodynamically attractive targets that are structurally inefficient or infeasible, although this is obtained at the cost of a larger design space and more expensive function evaluations.
The following sections formalize these two design optimization strategies and describe the aerodynamic and structural models used to evaluate the candidate airfoil shapes and compliant mechanisms.

### 2.1 Sequential Design Optimization of the Morphing Airfoil

The sequential Design Optimization process decomposes the morphing-airfoil design problem into two consecutive optimization stages. The first stage is an aerodynamic target-selection problem. It searches for a morphed airfoil geometry that improves aerodynamic efficiency, without evaluating the compliant mechanism required to produce that geometry. The second stage is a structural realization problem. It fixes the aerodynamic target selected in the first optimization stage and optimizes the compliant mechanism so that the prescribed target can be reproduced under aerodynamic and actuation loads.

**Aerodynamic Target Selection.** Let $\mathbf{z} \in \mathscr{Z}$ denote the aerodynamic design vector that parameterizes the target morphed airfoil shape $\mathbf{s_z}$. In the aerodynamic optimization stage, the optimizer minimizes the penalized negative lift-to-drag ratio of the target geometry:

$$\mathbf{z}_A^\star = \arg\min_{\mathbf{z}\in\mathscr{Z}} J_A(\mathbf{z}), \qquad J_A(\mathbf{z}) = -\frac{C_L(\mathbf{s_z})}{C_D(\mathbf{s_z})} + P_A(\mathbf{z}). \tag{1}$$

where $C_L(\mathbf{s_z})$ and $C_D(\mathbf{s_z})$ are the lift and drag coefficients computed for the target airfoil generated by $\mathbf{z}$. The penalization term $P_A(\mathbf{z})$ is used to represent aerodynamic and geometric inadmissibility, and the failure status of the aerodynamic solver:

$$\begin{aligned} P_A(\mathbf{z}) = {} & \rho_t \left[\max\left(0, t_{\text{req}} - t_{\min}(\mathbf{z})\right)\right]^2 + \rho_{\text{WB}} \left[\max\left(0, E_{\text{WB}}(\mathbf{z}) - E_{\text{WB,max}}\right)\right]^2 \\ & + \rho_{\ell,u} \left[\max\left(0, \frac{\left|\ell_{\text{TE},u}(\mathbf{z}) - \ell^0_{\text{TE},u}\right|}{\ell^0_{\text{TE},u}} - \delta_{\ell,u}\right)\right]^2 \\ & + \rho_{\ell,l} \left[\max\left(0, \frac{\left|\ell_{\text{TE},l}(\mathbf{z}) - \ell^0_{\text{TE},l}\right|}{\ell^0_{\text{TE},l}} - \delta_{\ell,l}\right)\right]^2 \\ & + \rho_A \left[\max\left(0, \frac{\left|A_{\text{TE}}(\mathbf{z}) - A^0_{\text{TE}}\right|}{A^0_{\text{TE}}} - \delta_A\right)\right]^2 \\ & + \rho_\kappa \left[\max\left(0, \kappa_{\text{TE,max}}(\mathbf{z}) - \kappa_{\max}\right)\right]^2 + \rho_{A,\text{fail}} \chi_A(\mathbf{z}). \end{aligned} \tag{2}$$

where $t_{\min}(\mathbf{z})$ is the minimum airfoil thickness of the target geometry and $t_{\text{req}}$ is the minimum admissible thickness; the quantity $E_{\text{WB}}(\mathbf{z})$ measures the deviation of the non-morphing wing-box region from the reference airfoil, while $E_{\text{WB,max}}$ is the maximum admissible value of this deviation; the quantities $\ell_{\text{TE},u}(\mathbf{z})$ and $\ell_{\text{TE},l}(\mathbf{z})$ are the upper and lower trailing-edge surface lengths of the target geometry, $\ell^0_{\text{TE},u}$ and $\ell^0_{\text{TE},l}$ are the corresponding reference values, and the parameters $\delta_{\ell,u}$ and $\delta_{\ell,l}$ define the admissible relative changes in these surface lengths; the term $A_{\text{TE}}(\mathbf{z})$ is the area of the morphing trailing-edge region, $A^0_{\text{TE}}$ is the corresponding reference value, and $\delta_A$ defines the admissible relative area variation; the quantity $\kappa_{\text{TE,max}}(\mathbf{z})$ is the maximum curvature of the target trailing-edge contour, and $\kappa_{\max}$ is the prescribed curvature limit. Finally, $\chi_A(\mathbf{z})$ is equal to one when the aerodynamic evaluation fails and zero otherwise. The coefficients $\rho_t$, $\rho_{\text{WB}}$, $\rho_{\ell,u}$, $\rho_{\ell,l}$, $\rho_A$, $\rho_\kappa$, and $\rho_{A,\text{fail}}$ are penalty weights. The penalty $P_A(\mathbf{z})$ does not contain any structural quantity, since the compliant mechanism is not evaluated during the aerodynamic stage. The aerodynamic design solution $\mathbf{z}^\star_A$ defines the aerodynamic target passed to the structural optimization stage.

**Structural Realization.** Let $\eta \in \mathscr{H}$ denote the structural design vector, which parameterizes the geometry, sizing, connectivity, and actuation variables of the compliant mechanism. The structural optimization problem is written as:

$$\eta^\star_S = \underset{\eta \in \mathscr{H}}{\arg\min}\, J_S(\eta; \mathbf{z}^\star_A), \tag{3}$$

where

$$J_S(\eta; \mathbf{z}^\star_A) = w_\varepsilon \varepsilon_{\text{shape}}(\mathbf{z}^\star_A, \eta) + w_W W_{\text{act}}(\mathbf{z}^\star_A, \eta) + w_m m(\eta) + P_S(\mathbf{z}^\star_A, \eta), \tag{4}$$

here, $\varepsilon_{\text{shape}}(\mathbf{z}^\star_A, \eta)$ measures the discrepancy between the fixed aerodynamic target and the realized loaded shape produced by the mechanism. The quantity $W_{\text{act}}(\mathbf{z}^\star_A, \eta)$ is the actuation work required to obtain the morphed configuration, while $m(\eta)$ is the structural mass. The coefficients $w_\varepsilon$, $w_W$, and $w_m$ define the relative importance assigned to target reproduction, actuation effort, and mass. The shape-tracking error $\varepsilon_{\text{shape}}(\mathbf{z}^\star_A, \eta)$ is introduced after the aerodynamic design solution $\mathbf{z}^\star_A$ has been obtained and reads as follows:

$$\varepsilon_{\text{shape}}(\mathbf{z}^\star_A, \eta) = \left[\frac{1}{N_s} \sum_{i=1}^{N_s} \left\| \mathbf{s}_{\text{real}\,i}(\mathbf{z}^\star_A, \eta) - \mathbf{s}_{\mathbf{z}i} \right\|_2^2\right]^{1/2}. \tag{5}$$

where $N_s$ is the number of comparison points in the morphing region, $\mathbf{s}_{\mathbf{z}i}$ is the $i$th point of the fixed target shape generated by $\mathbf{z}^\star_A$, and $\mathbf{s}_{\text{real}\,i}(\mathbf{z}^\star_A, \eta)$ is the corresponding point of the realized loaded geometry. The error therefore quantifies the ability of the compliant mechanism to reproduce the target selected by the aerodynamic optimizer.

The penalization term $P_S(\mathbf{z}_A^\star, \eta)$ is used to represent structural infeasibility and failed structural analyses:

$$\begin{aligned} P_S(\mathbf{z}_A^\star, \eta) = \rho_\sigma \left[\max\left(0, U_\sigma(\mathbf{z}_A^\star, \eta) - 1\right)\right]^2 + \rho_{\text{buck}} \left[\max\left(0, U_{\text{buck}}(\mathbf{z}_A^\star, \eta) - 1\right)\right]^2 \\ + \rho_F \left[\max\left(0, \frac{|F_{\text{act}}(\mathbf{z}_A^\star, \eta)|}{F_{\text{act,max}}} - 1\right)\right]^2 \\ + \rho_t \left[\max\left(0, t_{\min} - t_{\text{skin,min}}(\mathbf{z}_A^\star, \eta)\right)\right]^2 \\ + \rho_g \left[\max\left(0, g_{\min} - g_{\text{int}}(\mathbf{z}_A^\star, \eta)\right)\right]^2 + \rho_{S,\text{fail}} \chi_S(\mathbf{z}_A^\star, \eta). \end{aligned} \tag{6}$$

where $U_\sigma(\mathbf{z}_A^\star, \eta)$ is the maximum normalized stress utilization of the compliant mechanism and $U_{\text{buck}}(\mathbf{z}_A^\star, \eta)$ is the corresponding normalized buckling utilization, both normalized by their allowable values; the force $F_{\text{act}}(\mathbf{z}_A^\star, \eta)$ is the actuator force required by the structural solution, and $F_{\text{act,max}}$ is the prescribed actuator-force limit; the quantity $t_{\text{skin,min}}(\mathbf{z}_A^\star, \eta)$ is the minimum skin thickness associated with the candidate structural design, while $t_{\min}$ is the minimum admissible skin thickness; the quantity $g_{\text{int}}(\mathbf{z}_A^\star, \eta)$ denotes the minimum internal clearance between the compliant mechanism and the admissible airfoil envelope, and $g_{\min}$ is the prescribed clearance requirement. Finally, $\chi_S(\mathbf{z}_A^\star, \eta)$ is equal to one when the structural analysis fails or when the finite-element model does not return a physically meaningful loaded response, and zero otherwise. The coefficients $\rho_\sigma$, $\rho_{\text{buck}}$, $\rho_F$, $\rho_t$, $\rho_g$, and $\rho_{S,\text{fail}}$ are penalty weights.

**Final Sequential Design.** The final sequential design is denoted by $\mathbf{x}_{\text{seq}}^\star = (\mathbf{z}_A^\star, \eta_S^\star)$. Its aerodynamic performance must be evaluated carefully. The aerodynamic efficiency obtained in the first optimization stage refers only to the target geometry $\mathbf{s_z}$ and represents the nominal aerodynamic potential of the selected morphing shape. It does not represent the final physical performance of the aero-structural system. After the structural optimization stage, the compliant mechanism is loaded and actuated, the realized geometry $\mathbf{s}_{\text{real}}(\mathbf{z}_A^\star, \eta_S^\star)$ is reconstructed, and the aerodynamic model is applied again to this realized shape. The physically relevant lift-to-drag ratio of the sequential design is therefore

$$\frac{C_L\left(\mathbf{s}_{\text{real}}(\mathbf{z}_A^\star, \eta_S^\star)\right)}{C_D\left(\mathbf{s}_{\text{real}}(\mathbf{z}_A^\star, \eta_S^\star)\right)}.$$

This final evaluation separates the aerodynamic target selected by the first stage from the aerodynamic performance retained after structural realization. The sequential architecture is attractive from a computational standpoint because it decomposes the full aero-structural problem into two lower-dimensional optimization problems. This separation reduces the number of design variables handled at each stage, allows each disciplinary problem to be solved separately and avoids the need to evaluate a full aero-structural candidate at every iteration. In this sense, the sequential architecture provides a practical way to expose the aerodynamic potential of the morphing concept. However, this computational advantage comes with a loss of multidisciplinary consistency. The aerodynamic stage does not receive feedback from the structural model, and therefore it may select target shapes that are aerodynamically attractive but poorly aligned with the deformation modes and feasibility limits of the compliant mechanism. This trade-off between computational tractability and physical consistency motivates the coupled and architecture-aware formulations introduced in the following sections.

## 2.2 Coupled Formulation of the Morphing Airfoil

The coupled architecture removes the one-way separation between aerodynamic target selection and structural realization. Instead of first selecting an aerodynamic target and then designing a mechanism to reproduce it, the aerodynamic design vector $\mathbf{z}$ and the structural design vector $\eta$ are optimized simultaneously. Each candidate design therefore defines both a target morphed airfoil and the compliant mechanism intended to realize that target under load. The complete coupled design vector is written as $\mathbf{x} = (\mathbf{z}, \eta)$, with $\mathbf{z} \in \mathscr{Z}$ and $\eta \in \mathscr{H}$.

For a given candidate $\mathbf{x}$, the aerodynamic variables define the target morphed shape $\mathbf{s_z}$. This target is used to compute the aerodynamic loading applied to the structural model. The structural model

then evaluates the loaded deformation of the compliant mechanism defined by $\eta$, producing the realized geometry $\mathbf{s}_{\text{real}}(\mathbf{z},\eta)$. The aerodynamic performance of the candidate is finally evaluated on this realized geometry, rather than on the target geometry alone. The coupled optimization problem is written as:

$$\mathbf{x}_C^\star = \underset{\mathbf{z}\in\mathscr{Z},,\eta\in\mathscr{H}}{\arg\min}\ J_C(\mathbf{z},\eta), \tag{7}$$

where

$$J_C(\mathbf{z},\eta) = -\frac{C_L\left(\mathbf{s}_{\text{real}}(\mathbf{z},\eta)\right)}{C_D\left(\mathbf{s}_{\text{real}}(\mathbf{z},\eta)\right)} + w_\varepsilon \varepsilon_{\text{shape}}(\mathbf{z},\eta) + w_W W_{\text{act}}(\mathbf{z},\eta) + w_m m(\eta) + P_A(\mathbf{z},\eta) + P_S(\mathbf{z},\eta). \tag{8}$$

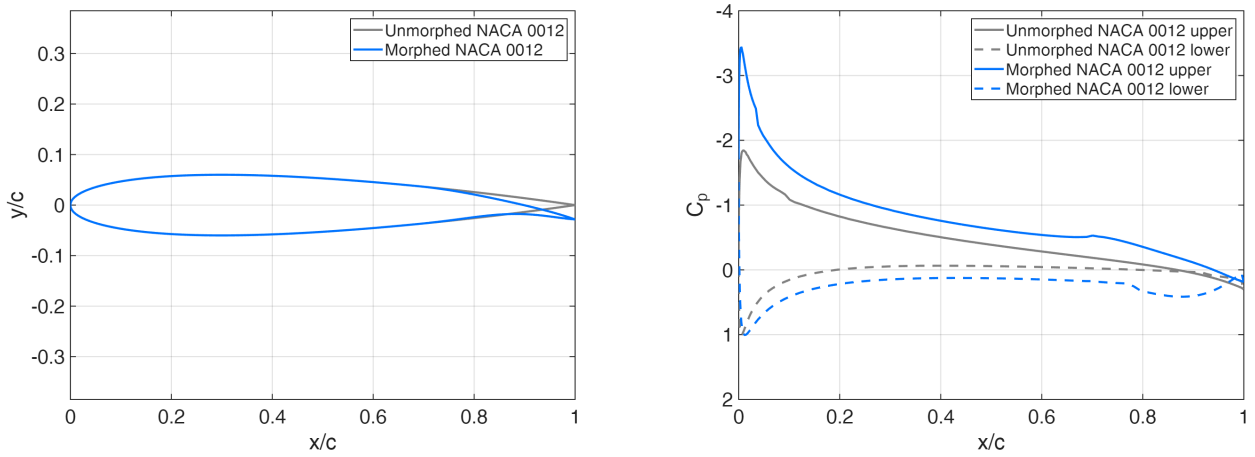
where $\mathbf{x}_C^\star$ denotes the optimal coupled design. The first term in Eq. (8) is the negative lift-to-drag ratio computed on the realized loaded shape $\mathbf{s}_{\text{real}}(\mathbf{z},\eta)$. Thus, unlike the sequential aerodynamic stage, the aerodynamic coefficients are evaluated on the geometry produced by the compliant mechanism after loading and actuation, rather than on the target geometry alone. The remaining objective terms retain the same meaning introduced in the sequential formulation. The quantities $\varepsilon_{\text{shape}}(\mathbf{z},\eta)$, $W_{\text{act}}(\mathbf{z},\eta)$, and $m(\eta)$ account for target tracking, actuation effort, and structural mass, respectively, while $w_\varepsilon$, $w_W$, and $w_m$ define their relative weights. The penalty terms also preserve the disciplinary interpretation defined previously: $P_A(\mathbf{z},\eta)$ accounts for aerodynamic and geometric inadmissibility, whereas $P_S(\mathbf{z},\eta)$ accounts for structural feasibility violations and failed structural analyses.

**Coupled Design.** The coupled formulation changes the role of the aerodynamic target. In the sequential architecture, the target shape is fixed after the aerodynamic stage, and the structural optimizer can only search for the best feasible mechanism to reproduce it. In the coupled architecture, the target shape remains part of the optimization process. If a target geometry is aerodynamically attractive but difficult to realize, the optimizer can move toward a different target that provides a better balance between realized aerodynamic efficiency, shape tracking, actuation effort, mass, and structural feasibility. This increased physical consistency comes with a loss of computational tractability. The coupled optimizer acts on the combined design vector rather than on two smaller disciplinary design spaces solved in sequence. The search therefore has to explore aerodynamic shape variables together with structural geometry, sizing, connectivity, and actuation variables. This increases the dimensionality of the optimization problem and also makes the feasible region more difficult to identify, because an admissible design must satisfy aerodynamic, geometric, and structural requirements at the same time.

The cost of each function evaluation is also higher than in the sequential disciplinary stages. Each coupled candidate requires the generation of a target airfoil, an aerodynamic evaluation of the target shape to obtain the aerodynamic loading, a loaded structural analysis to compute the realized geometry, and a second aerodynamic evaluation on the realized shape. The coupled formulation is therefore more representative of the physical design problem, because the value of a target shape is judged through the geometry that the loaded compliant mechanism can actually produce. However, this representativeness is obtained by replacing two lower-dimensional disciplinary searches with a single higher-dimensional, more expensive, and more constrained aero-structural design search. This trade-off motivates the architecture-aware strategy introduced next, which aims to retain the physical relevance of coupled evaluations while reducing the number of fully coupled evaluations required during the search.

## 2.3 Aerodynamic Model

The aerodynamic model maps the aerodynamic design vector $\mathbf{z}$ into a target morphed airfoil and evaluates the corresponding aerodynamic response. The aerodynamic design vector $\mathbf{z}$ contains eight CST perturbation coefficients: four coefficients modify the upper surface of the morphing region and four coefficients modify the lower surface. These perturbations are applied only in the aft portion of the airfoil, while the forward non-morphing region is preserved for structural compatibility. The primary role of the aerodynamic model is to provide the lift and drag coefficients used in the aerodynamic objective, together with the surface pressure distribution required to load the structural model. The same aerodynamic model is used in all optimization architectures.




(a) Reference and morphed NACA 0012.

(b) Pressure-coefficient distributions.

Figure 1 – Aerodynamic model output for reference and morphed NACA 0012 airfoils: figure 1a shows the CST-based trailing-edge morphing, while figure 1b shows the corresponding XFOIL pressure-coefficient distributions.

The target geometry is represented using a Class-Shape Transformation parameterization [25]. For each airfoil surface, the non-dimensional chordwise coordinate is denoted by $\psi$, and the corresponding non-dimensional surface ordinate is denoted by $\zeta(\psi)$. The surface representation is written as:

$$\zeta(\psi) = \psi^{N_1}(1-\psi)^{N_2} \sum_{i=0}^{N_{\mathrm{CST}}-1} A_i B_i(\psi) + \psi \Delta\xi_{\mathrm{TE}}. \tag{9}$$

where $N_1$ and $N_2$ are the class-function exponents, $A_i$ are the CST coefficients, $B_i(\psi)$ denotes the standard Bernstein basis function of order $N_{\mathrm{CST}}-1$, $N_{\mathrm{CST}}$ is the number of CST coefficients, and $\Delta\xi_{\mathrm{TE}}$ is the trailing-edge thickness term. Separate coefficient sets are assigned to the upper and lower surfaces, allowing the target parameterization to modify camber and thickness in the morphing region while preserving the prescribed non-morphing portion of the airfoil.

The aerodynamic analysis is performed using XFOIL [26] and computes the lift coefficient $C_L(\mathbf{s_z})$, the drag coefficient $C_D(\mathbf{s_z})$, and the surface pressure distribution associated with the target airfoil $\mathbf{s_z}$. The quantities entering the penalty term $P_A(\mathbf{z})$ are obtained from the target geometry and from the XFOIL convergence status.

Figure 1 illustrates the aerodynamic evaluation used in the optimization loop for a representative morphed configuration. The XFOIL analyses are performed at Reynolds $Re = 3.5 \times 10^6$, Mach $M = 0.15$, and angle of attack $\alpha = 5°$. Figure 1a compares the reference NACA 0012 profile with the morphed target geometry generated by the CST perturbation of the aft region. Figure 1b reports the corresponding pressure-coefficient distributions on the upper and lower surfaces. The change in the aft geometry modifies the pressure loading over the airfoil, which is then used to construct the aerodynamic load vector transferred to the structural model.

## 2.4 Structural Model

The structural model evaluates the response and feasibility of the compliant mechanism associated with a prescribed target morphing shape. The mechanism is represented by a two-dimensional beam-network finite-element model embedded in the trailing-edge region of the airfoil. In the present implementation, the primary morphing kinematics are prescribed by a trailing-edge deformation map. The structural design vector $\eta$ parameterizes the prescribed compliant trailing-edge mechanism through nine normalized variables; the first group controls the actuation level and the maximum trailing-edge rotation used to construct the morphed kinematics; the second group controls the relative upper and lower input motions and the internal height of the mechanism, which determine how the actuation is transmitted through the beam network; the remaining variables define the cross-sectional dimensions of the skin, internal links, ribs, and trailing-edge cap. The mechanism topology

is fixed: the rib stations, beam connectivity, rear-spar attachment, and trailing-edge cap layout are prescribed by the selected architecture.

For a given aerodynamic design $\mathbf{z}$, the target airfoil shape $\mathbf{s_z}$ is first evaluated aerodynamically. The pressure distribution computed on the target geometry is transferred to the trailing-edge skin nodes and used to define the aerodynamic loads acting on the compliant mechanism. The realized external contour is generated through a prescribed kinematic map:

$$\mathbf{s}_{\text{real}}(\mathbf{z},\eta) = \mathscr{G}\left(\mathbf{s}_{\mathbf{z}},\eta\right), \tag{10}$$

where $\mathscr{G}$ represents the deformation rule that maps the target airfoil and the structural design parameters into the realized geometry. The rear-spar region remains fixed and provides the attachment to the non-morphing part of the airfoil.

The beam-network model evaluates the strain induced by the prescribed morphing deformation and the additional stress contribution associated with the mapped aerodynamic loads. For each beam member $e$, the axial morphing strain is computed from the neutral and morphed member lengths:

$$\varepsilon_e^{\text{morph}} = \frac{L_e(\eta) - L_{e,0}}{L_{e,0}}, \tag{11}$$

where $L_{e,0}$ and $L_e(\eta)$ are the neutral and morphed lengths of member $e$. The corresponding stress contribution is combined with the load-induced axial and bending stress estimates obtained from the aerodynamic loads.

The actuation model is represented by an equivalent antagonistic input pair acting through upper and lower input points. Let $\mathbf{r}_{u,0}$ and $\mathbf{r}_{l,0}$ denote the neutral upper and lower input points, and let $\mathbf{r}_u$ and $\mathbf{r}_l$ denote their actuated positions. The relative actuation stroke is defined as:

$$s_{\text{rel}}(\eta) = \left\|(\mathbf{r}_u - \mathbf{r}_{u,0}) - (\mathbf{r}_l - \mathbf{r}_{l,0})\right\|_2. \tag{12}$$

The corresponding equivalent actuator force and actuation work are computed as:

$$F_{\text{act}}(\eta) = k_{\text{act}} s_{\text{rel}}(\eta), \qquad W_{\text{act}}(\mathbf{z},\eta) = \frac{1}{2} k_{\text{act}} s_{\text{rel}}^2(\eta), \tag{13}$$

where $k_{\text{act}}$ is the equivalent actuator stiffness. This quasi-static model quantifies the actuation effort associated with the prescribed input motion.

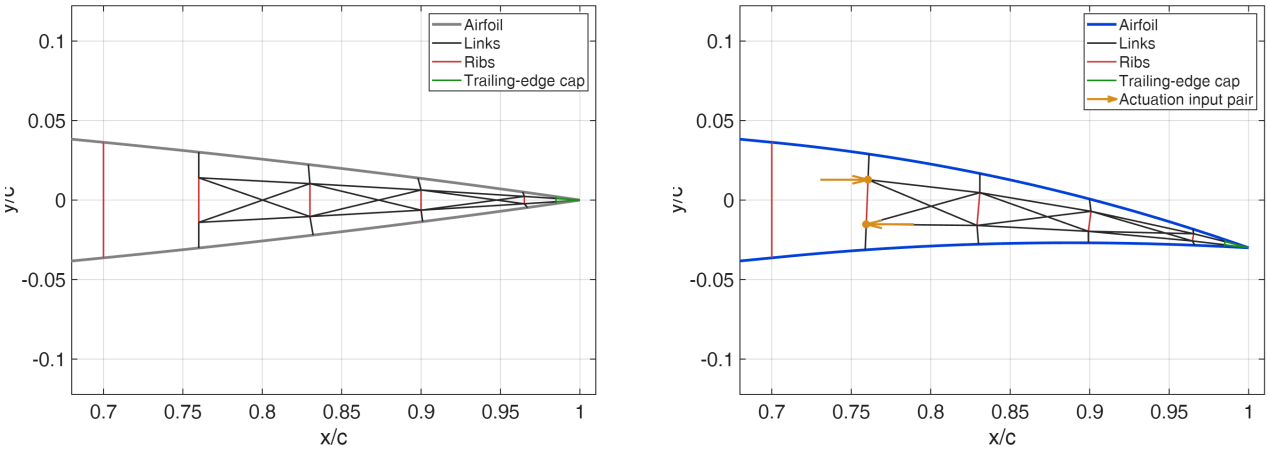
The structural model also computes the structural mass, and the penalty term $P_S(\mathbf{z}_A^\star,\eta)$ including stress and buckling utilization of the beam-network mechanism, minimum skin thickness and minimum internal clearance between the compliant mechanism and the admissible airfoil envelope.

Figure 2 illustrates the structural representation for a representative compliant trailing-edge mechanism. Figure 2a shows the reference configuration of the beam-network model embedded within the trailing-edge region. The external airfoil contour, internal links, ribs, and trailing-edge cap define the neutral mechanism layout before actuation. Figure 2b shows the corresponding morphed configuration generated by the prescribed kinematic map. The arrows indicate the equivalent antagonistic actuation input pair used to prescribe the mechanism motion.

## 3. Architecture-Aware Bayesian Optimization

The previous section introduced the sequential and coupled formulations of the trailing-edge morphing airfoil design problem. The sequential formulation is computationally attractive because aerodynamic target selection and structural realization are solved separately, reducing the dimensionality and cost of each search stage. Its limitation is that the aerodynamic target is selected before structural feasibility and loaded shape recovery are assessed. The coupled formulation evaluates each candidate through the geometry realized by the loaded compliant mechanism, and is therefore closer to the physical design objective. This improvement in consistency is obtained at a higher computational cost, because each candidate requires the full aero-structural evaluation chain.

This section introduces a novel architecture-aware Bayesian optimization strategy designed to adapt the level of aero-structural coupling during the search. Rather than committing a priori to either




(a) Reference configuration.

(b) Morphed configuration.

Figure 2 – Representative structural model configurations for the compliant trailing-edge mechanism. The reference configuration in figure 2a defines the neutral beam-network layout embedded within the airfoil, while the morphed configuration 2b shows the corresponding realized geometry used in the loaded structural assessment.

a sequential or fully coupled optimization process, the method decides during the search when a lower-cost sequential-type evaluation is sufficient and when a full coupled evaluation is required to resolve the realized aerodynamic response.

The proposed methodology is rooted in Bayesian optimization for expensive to evaluate black box objective functions [27, 28], where a surrogate model provides both a prediction of the objective and an uncertainty estimate, and an acquisition function selects the next query by balancing exploitation and exploration. Our architecture-aware Bayesian optimization extends this logic to the morphing wing design problem by allowing the optimizer to select not only the next candidate design, but also the aero-structural evaluation chain used to query that candidate. It is therefore designed to approach the physical relevance of a coupled search without requiring every candidate to be evaluated through the full coupled chain.

The evaluation choices are defined at the level of a complete candidate design $\mathbf{x} = (\mathbf{z}, \eta)$. The sequential-type evaluation computes the target aerodynamics associated with $\mathbf{z}$, transfers the corresponding pressure loading to the structural model, and evaluates the loaded structural response of the mechanism defined by $\eta$. This evaluation returns the sequential-type objective $J_{\text{seq}}(\mathbf{x})$, which combines the aerodynamic performance of the target shape with the structural realization metrics, but does not recompute the aerodynamic performance on the realized geometry. The coupled evaluation instead evaluates the candidate $\mathbf{x}$ through the complete aero-structural chain and returns the coupled objective $J_C(\mathbf{x})$, where the aerodynamic performance is computed on the realized geometry $\mathbf{s}_{\text{real}}(\mathbf{z}, \eta)$.

Within the proposed architecture-aware Bayesian optimization framework, the surrogate model represents both the sequential-type objective $J_{\text{seq}}$ and the discrepancy between sequential-type and coupled evaluations, defined as $\Delta_C = J_C - J_{\text{seq}}$. The acquisition function uses the predicted response, the associated uncertainty, the discrepancy information, and the relative evaluation cost to select whether the next query should be performed with the sequential-type evaluation or with the full coupled evaluation. The following subsections describe the surrogate model and the architecture-aware acquisition function used to guide this selection.

## 3.1 Surrogate Model

The surrogate model is built around two quantities defined on the complete aero-structural design vector $\mathbf{x} = (\mathbf{z}, \eta)$. The first is the sequential-type objective $J_{\text{seq}}(\mathbf{x})$, which evaluates the target aerodynamics and the loaded structural realization of the candidate. The second is the discrepancy $\Delta_C(\mathbf{x})$ between the sequential-type and coupled evaluations.

The sequential-type objective is obtained by combining the aerodynamic target objective with the structural objective defined in the sequential formulation $J_{\text{seq}}(\mathbf{x}) = J_A(\mathbf{z}) + J_S(\eta;\mathbf{z})$, where the aerodynamic contribution $J_A(\mathbf{z})$ is the target-geometry objective defined in Eq. (1) and the structural contribution $J_S(\eta;\mathbf{z})$ is the loaded-realization objective defined in Eq. (4)
The discrepancy between the coupled and sequential-type evaluations is defined as $\Delta_C(\mathbf{x}) = J_C(\mathbf{x}) - J_{\text{seq}}(\mathbf{x})$ where the quantity $\Delta_C$ measures the correction required to recover the coupled objective from the sequential-type objective. Since the problem is written in minimization form, a positive value of $\Delta_C$ indicates that the sequential-type evaluation is optimistic with respect to the coupled evaluation, whereas a negative value indicates that it is conservative for that design.
The available observations are organized into two datasets. The dataset $\mathscr{D}_{\text{seq}}$ contains pairs of the form $(\mathbf{x}_i, J_{\text{seq}}(\mathbf{x}_i))$ and is populated by sequential-type evaluations, as well as by the sequential-type values also available from coupled evaluations. The dataset $\mathscr{D}_\Delta$ contains pairs of the form $(\mathbf{x}_i, \Delta_C(\mathbf{x}_i))$ and is populated only by coupled evaluations.
Two Gaussian Process (GP) regression models are used [29, 30]. The first GP approximates the sequential-type objective:

$$J_{\text{seq}}(\mathbf{x}) \sim \mathscr{GP}\left(m_{\text{seq}}(\mathbf{x}), k_{\text{seq}}(\mathbf{x},\mathbf{x}')\right), \tag{14}$$

and the second GP models the discrepancy:

$$\Delta_C(\mathbf{x}) \sim \mathscr{GP}\left(m_\Delta(\mathbf{x}), k_\Delta(\mathbf{x},\mathbf{x}')\right). \tag{15}$$

where the covariance functions $k_{\text{seq}}$ and $k_\Delta$ use squared-exponential kernels.
Conditioning the two GP priors on their corresponding datasets gives the posterior predictive distributions:

$$J_{\text{seq}}(\mathbf{x}) \mid \mathscr{D}_{\text{seq}} \sim \mathscr{N}\left(\mu_{\text{seq}}(\mathbf{x}), \sigma^2_{\text{seq}}(\mathbf{x})\right), \tag{16}$$

and

$$\Delta_C(\mathbf{x}) \mid \mathscr{D}_\Delta \sim \mathscr{N}\left(\mu_\Delta(\mathbf{x}), \sigma^2_\Delta(\mathbf{x})\right). \tag{17}$$

where the predictive means $\mu_{\text{seq}}$ and $\mu_\Delta$ estimate the sequential-type objective and the coupled correction, while $\sigma_{\text{seq}}$ and $\sigma_\Delta$ quantify the corresponding predictive uncertainties.
The coupled objective is predicted through the sequential-discrepancy decomposition,

$$J_C(\mathbf{x}) = J_{\text{seq}}(\mathbf{x}) + \Delta_C(\mathbf{x}). \tag{18}$$

The corresponding predictive mean is:

$$\mu_C(\mathbf{x}) = \mu_{\text{seq}}(\mathbf{x}) + \mu_\Delta(\mathbf{x}), \tag{19}$$

while the predictive variance is approximated as:

$$\sigma^2_C(\mathbf{x}) = \sigma^2_{\text{seq}}(\mathbf{x}) + \sigma^2_\Delta(\mathbf{x}). \tag{20}$$

This variance approximation treats the sequential-type and discrepancy prediction errors as independent. The resulting surrogate allows lower-cost sequential-type evaluations to guide the search through $J_{\text{seq}}$, while coupled evaluations learn the correction $\Delta_C$ required to estimate the physically relevant objective $J_C$.

## 3.2 Architecture-Aware Acquisition Function

The surrogate model provides the predictive mean and standard deviation of the sequential-type objective, $\mu_{\text{seq}}(\mathbf{x})$ and $\sigma_{\text{seq}}(\mathbf{x})$, and of the discrepancy, $\mu_\Delta(\mathbf{x})$ and $\sigma_\Delta(\mathbf{x})$. The acquisition function uses these predictions to decide which design candidate should be queried and whether the candidate should be evaluated with the lower-cost sequential-type evaluation or with the full coupled evaluation. We measure the design improvement at each iteration through acquisition scores based on expected improvement acquisition function defined as [31]:

$$\text{EI}(\mu,\sigma;J^{\min}) = \left(J^{\min} - \mu\right)\Phi(\gamma) + \sigma\phi(\gamma), \qquad \gamma = \frac{J^{\min} - \mu}{\sigma}. \tag{21}$$

where $\phi$ and $\Phi$ are the probability density and cumulative distribution functions of the standard normal distribution.

For each candidate design $\mathbf{x}$, we define two acquisition scores: one associated with the sequential-type evaluation and one associated with the coupled evaluation. For the sequential-type evaluation, the score is computed from the GP prediction of $J_{\text{seq}}$:

$$S_{\text{seq}}(\mathbf{x}) = \frac{\text{EI}\left(\mu_{\text{seq}}(\mathbf{x}), \sigma_{\text{seq}}(\mathbf{x}); J_{\text{seq}}^{\min}\right)}{c_{\text{seq}}}. \tag{22}$$

where $J_{\text{seq}}^{\min}$ is the best sequential-type objective observed so far and the cost $c_{\text{seq}}$ corresponds to one sequential-type evaluation, including the aerodynamic analysis of the target geometry and loaded structural analysis. The score $S_{\text{seq}}$ favors candidates that are promising under the lower-cost evaluation, which combines target aerodynamic performance and loaded structural realization without recomputing the aerodynamic performance on the realized geometry.

For the coupled evaluation, the score is computed from the predicted coupled objective obtained through the sequential-discrepancy surrogate. A coupled evaluation provides two pieces of information: the value of the physically relevant objective $J_C(\mathbf{x})$ and the discrepancy $\Delta_C(\mathbf{x})$ between the sequential-type and coupled evaluations at the same candidate.

The acquisition score therefore includes both an improvement term and a discrepancy-learning term:

$$S_C(\mathbf{x}) = \frac{\text{EI}\left(\mu_C(\mathbf{x}), \sigma_C(\mathbf{x}); J_C^{\min}\right) + \lambda_\Delta \sigma_\Delta(\mathbf{x})}{c_C}. \tag{23}$$

where $J_C^{\min}$ is the best coupled objective observed so far and the cost $c_C$ corresponds to one full coupled evaluation, which includes the same sequential operations and the additional aerodynamic analysis of the realized geometry. The expected-improvement term favors candidates predicted to reduce the physically relevant coupled objective. The second term, $\lambda_\Delta \sigma_\Delta(\mathbf{x})$, assigns additional value to coupled evaluations in regions where the discrepancy model is uncertain. The coefficient $\lambda_\Delta$ controls the relative importance assigned to learning this correction.

The next candidate is selected by maximizing, over the complete design space, the larger of the two cost-normalized acquisition scores:

$$\mathbf{x}_{t+1} = \underset{\mathbf{x} \in \mathscr{X} \times \mathscr{H}}{\arg\max} \left[\max\left(S_{\text{seq}}(\mathbf{x}), S_C(\mathbf{x})\right)\right]. \tag{24}$$

If $S_{\text{seq}}(\mathbf{x}_{t+1}) \geq S_C(\mathbf{x}_{t+1})$, the selected candidate is evaluated with the sequential-type model. Otherwise, the coupled evaluation is performed. The evaluation architecture is therefore determined by the score that attains the maximum at the selected design.

The architecture-aware property of the method is embedded in the acquisition step because the optimizer compares two scores associated with two different evaluation chains. The sequential-type score assigns value to evaluating a candidate through target aerodynamics and loaded structural realization, while the coupled score assigns value to evaluating the same design class through the full chain in which aerodynamic performance is recomputed on the realized geometry. The architecture used at the next iteration is therefore selected by the optimization process itself. This makes the method architecture-aware in a precise sense: the optimizer is aware that the same candidate can be queried at different levels of aero-structural coupling, with different cost and information content, and therefore adapts the evaluation architecture during the search, rather than committing a priori to either a sequential or fully coupled optimization strategy.

## 4. Results and Discussion

This section investigates the performance of the proposed architecture-aware Bayesian optimization strategy for the design of the trailing-edge morphing airfoil introduced in the previous sections. The objective is to assess whether the architecture-aware search can retain the physical relevance of the coupled formulation while reducing the computational effort associated with repeated full aero-structural evaluations. The comparison is carried out against the two optimization architectures introduced in Section 2.: the sequential formulation (Section 2.1), in which aerodynamic target selection and structural realization are optimized in two separate stages, and the coupled formulation (Section 2.2), in which the aerodynamic and structural design variables are optimized simultaneously.

## 4.1 Experimental Settings

For the sequential and coupled formulations, the design problems are solved using a standard Efficient Global Optimization (EGO) BO strategy based on Gaussian process regression and the expected-improvement acquisition function [31]. In the sequential case, the EGO procedure is applied first to the aerodynamic target-selection problem and then to the structural realization problem. In the coupled case, the same EGO procedure is applied directly to the complete aero-structural design vector. The architecture-aware strategy follows the formulation introduced in Section 3., where the acquisition function selects between a lower-cost sequential-type evaluation and a full coupled evaluation during the search. In the following, sequential BO refers to the EGO solution of the sequential formulation, coupled BO refers to the EGO solution of the coupled formulation, and architecture-aware BO refers to the proposed evaluation-aware strategy.

All aerodynamic evaluations are performed under the same two-dimensional flight condition. The airfoil is analysed at a Reynolds number of $Re = 3.5 \times 10^6$, Mach number $M = 0.15$, and angle of attack $\alpha = 5^\circ$. These conditions are used consistently for the target aerodynamic evaluations and for the final aerodynamic evaluation of the realized loaded geometry. Therefore, differences in $(C_L/C_D)_{\text{real}}$ arise from the optimization architecture and from the target-to-realized geometry discrepancy, rather than from changes in the operating condition.

All comparisons are performed on the realized loaded geometry, since this is the configuration that determines the physical aerodynamic performance of the morphing airfoil. The reported aerodynamic metric is the realized lift-to-drag ratio $(C_L/C_D)_{\text{real}}$ computed after the compliant mechanism has produced the loaded shape. The remaining quantities characterize the structural realization of the design, including the shape-tracking error $\varepsilon_{\text{shape}}$, the actuation work $W_{\text{act}}$, the structural mass $m$, and the stress and buckling utilizations $U_\sigma$ and $U_{\text{buck}}$. The cost at the best design is the cumulative evaluation cost spent up to the iteration in which the best design of a run is first obtained. It is computed by summing the prescribed cost of each model evaluation performed before that point, from the first evaluation up to the first iteration at which the best realized design is found. In the present study, the normalized costs are set to $c_{\text{seq}} = 0.5$ for a sequential-type structural realization evaluation, and $c_C = 1$ for a full coupled evaluation. These values reflect the relative expense of the evaluation chains and are used only as a consistent computational-budget measure across the compared optimization architectures.

The initial designs are generated through Latin hypercube sampling in the corresponding design spaces. The sequential BO baseline uses $30$ initial samples while the coupled BO baseline uses $15$ initial evaluations. The architecture-aware BO strategy is initialized with $10$ sequential-type evaluations, and $10$ coupled evaluations. This gives comparable initial sampling effort across the three methods while reflecting the different structure of the corresponding optimization processes. The same surrogate-modeling and acquisition-function settings are used across the compared methods, so that differences in performance can be attributed to the optimization architecture rather than to different Bayesian optimization parameters. The comparison is repeated over ten independent runs to account for the stochasticity associated with the initial sampling and candidate-generation process.

## 4.2 Discussion

Figure 3 compares the realized aerodynamic efficiency obtained in the ten runs of each method against the cost required to reach the best design in the corresponding run. The sequential BO results are concentrated at moderate computational cost, but their realized aerodynamic efficiencies remain generally lower than those obtained by the coupled and architecture-aware searches. This is consistent with the sequential formulation: the aerodynamic target is selected before structural realization is considered, and the final geometry produced by the compliant mechanism may not retain the aerodynamic performance of the target shape.

The coupled BO results achieve the highest realized aerodynamic efficiencies, with most runs located close to or above $(C_L/C_D)_{\text{real}} = 100$. This reflects the benefit of retaining the aero-structural coupling within the optimization loop. However, the same figure also shows that these values are obtained at substantially larger cost. This behavior follows directly from the coupled evaluation chain, where each candidate requires the target aerodynamic evaluation, the loaded structural analysis, and the

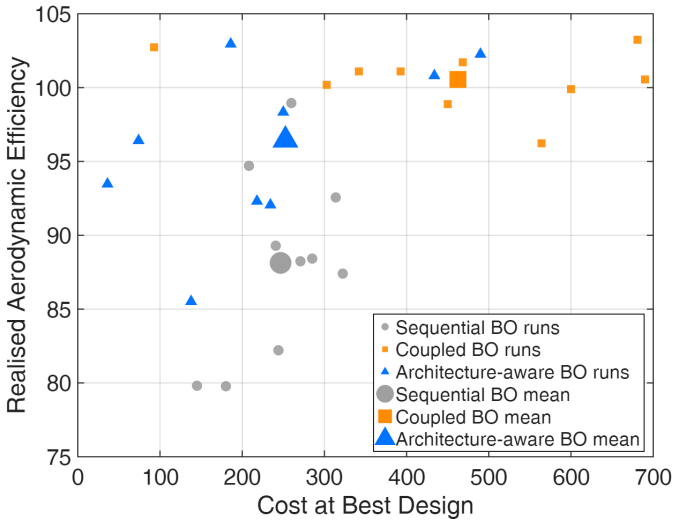



Figure 3 – Realized aerodynamic efficiency as a function of the cost at the best design for the sequential BO, coupled BO and Architecture-aware BO over ten independent runs. Small markers indicate individual runs, while larger markers indicate the corresponding median values.

Table 1 – Statistical comparison of the three optimization architectures over ten independent runs. The reported quantities are computed on the realised loaded geometry. Values are reported as median.

| Method - Median Design | $(C_L/C_D)_{\text{real}}$ | $\varepsilon_{\text{shape}}$ [mm] | $W_{\text{act}}$ [J] | $m$ [kg] | $U_\sigma$ | $U_{\text{buck}}$ | Cost |
|---|---|---|---|---|---|---|---|
| Sequential BO | 88.33 | 5.20 | 2.50 | 1.64 | 0.099 | 0.317 | 252.0 |
| Coupled BO | 100.82 | 6.19 | 12.21 | 2.08 | 0.488 | 0.438 | 459.0 |
| Architecture-aware BO | 97.37 | 6.36 | 8.20 | 2.77 | 0.285 | 0.386 | 226.0 |

Table 2 – Best design obtained by each optimization architecture. The best design is selected according to the final coupled objective, while the table reports the corresponding realised aerodynamic performance and structural quantities.

| Method - Best Design | $(C_L/C_D)_{\text{real}}$ | $\varepsilon_{\text{shape}}$ [mm] | $W_{\text{act}}$ [J] | $m$ [kg] | $U_\sigma$ | $U_{\text{buck}}$ | Cost |
|---|---|---|---|---|---|---|---|
| Sequential BO | 98.96 | 4.89 | 33.27 | 1.66 | 0.361 | 0.877 | 260.0 |
| Coupled BO | 103.23 | 5.54 | 13.89 | 1.68 | 0.795 | 0.606 | 581.0 |
| Architecture-aware BO | 102.25 | 4.25 | 11.79 | 1.59 | 0.637 | 0.424 | 290.0 |

aerodynamic evaluation of the realized shape.

The architecture-aware BO results occupy the region between these two limiting behaviors. The method reaches realized aerodynamic efficiencies close to those obtained by the coupled formulation, while requiring a substantially smaller cost at the best design. This indicates that the architecture-aware strategy is able to exploit the sequential-type evaluation as informative lower-cost evidence, while using coupled evaluations to correct the prediction when the realized aerodynamic performance becomes relevant for the search.

Table 1 reports the median results over the ten independent runs. The sequential BO architecture reaches a median $(C_L/C_D)_{\text{real}}$ of $88.33$, while the coupled BO architecture reaches $100.82$. The architecture-aware BO strategy obtains a median $(C_L/C_D)_{\text{real}}$ of $97.37$, corresponding to a $10.2\%$ improvement over sequential BO. This value remains only $3.4\%$ below the coupled BO median and recovers approximately $72.4\%$ of the aerodynamic-efficiency gain obtained by moving from the sequential to the coupled formulation. The corresponding median cost at the best design is $226.0$ for architecture-aware BO, compared with $252.0$ for sequential BO and $459.0$ for coupled BO. Thus, architecture-aware BO reduces the median cost by $50.8\%$ with respect to coupled BO. The method therefore captures most of the aerodynamic benefit associated with coupled evaluations while avoiding the systematic use of the full coupled chain.

The structural quantities in Table 1 indicate that all median designs remain within the admissible stress and buckling limits. The sequential BO design has the lowest median stress and buckling utilizations, but this conservative structural response is accompanied by the lowest realized aerodynamic efficiency. The coupled BO design improves the realized aerodynamic performance, but at the expense of larger actuation work and higher stress utilization. The architecture-aware BO design gives intermediate values of actuation work and utilization, while maintaining an aerodynamic efficiency close to the coupled formulation. This reflects the intended role of the architecture-aware policy: the search is not driven only by the lower-cost sequential-type evaluations, but it also does not require every candidate to be evaluated with the full coupled chain.

Table 2 reports the best design obtained by each search method and architecture. The coupled BO architecture gives the highest realized aerodynamic efficiency, with $(C_L/C_D)_{\text{real}} = 103.23$, but this design is obtained at a cost of $581.0$. The architecture-aware BO strategy obtains $(C_L/C_D)_{\text{real}} = 102.25$, which is only $0.9\%$ lower than the coupled BO best design and $3.3\%$ higher than the sequential BO best design. This performance is achieved at a cost of $290.0$, corresponding to a $50.1\%$ reduction with respect to coupled BO, although it remains $11.5\%$ higher than the cost required by the sequential BO best design.

The architecture-aware best design also provides favorable structural-realization metrics. Its shape-tracking error is $4.25$ mm, corresponding to a $13.1\%$ reduction with respect to sequential BO and a $23.3\%$ reduction with respect to coupled BO. Its actuation work is $11.79$ J, which is $64.6\%$ lower than the value obtained by sequential BO and $15.1\%$ lower than the value obtained by coupled BO. The structural mass is also the lowest among the three best designs, with $m = 1.59$ kg, corresponding to reductions of $4.2\%$ and $5.4\%$ with respect to sequential BO and coupled BO, respectively. The stress utilization of the architecture-aware best design is higher than that of sequential BO, but remains below the admissible limit, while its buckling utilization is reduced by $51.7\%$ with respect to sequential BO and by $30.0\%$ with respect to coupled BO. These results indicate that the architecture-aware strategy identifies a design that is close to the coupled optimum in realized aerodynamic efficiency, while requiring substantially lower computational cost and improving several structural-realization metrics.

**Remarks.** These results indicate that architecture-aware BO closes much of the gap between sequential and coupled optimization without paying the cost of a fully coupled search. The method reaches coupled-level realized aerodynamic efficiency with substantially fewer full coupled evaluations, while preserving competitive shape recovery, actuation work, and structural utilization. This is the central advantage for morphing-airfoil design: the optimizer must not only identify an aerodynamically efficient target shape, but also determine whether that shape can be produced by a compliant mechanism under load without losing its aerodynamic value. By learning the discrepancy between the sequential-type and coupled evaluations during the search, the architecture-aware strategy uses the lower-cost sequential evaluation where it is informative and reserves full coupled evaluations for designs whose value must be judged on the realized geometry. This leads to an optimization process that remains connected to the physical aero-structural response without incurring the cost of evaluating every candidate through the full coupled chain.

## 5. Conclusions

This work proposed an architecture-aware Bayesian optimization strategy for the multidisciplinary design optimization of a trailing-edge morphing airfoil equipped with an internal compliant mechanism. The method addresses the trade-off between the computational tractability of the sequential MDO formulation and the physical consistency of the coupled MDO formulation.

The proposed architecture-aware Bayesian optimization strategy retains the coupled objective as the physically relevant design criterion, while using lower-cost sequential-type evaluations as informative approximations during the search. This is achieved by learning the sequential-type objective and the discrepancy between sequential-type and coupled evaluations. The acquisition function then decides whether the next candidate should be evaluated through the lower-cost sequential-type chain or through the full coupled chain. In this way, the optimization process does not commit a priori to

either a purely sequential or a fully coupled search strategy, but adapts the evaluation architecture to the information required by the current surrogate state.

The experimental results show that the architecture-aware strategy captures most of the aerodynamic benefit of the coupled MDO formulation at substantially reduced computational cost. Over ten independent runs, architecture-aware BO improves the median realized lift-to-drag ratio by approximately $10\%$ with respect to sequential BO, while remaining only about $3\%$ below coupled BO. At the same time, the median cost at the best design is reduced by about $51\%$ with respect to coupled BO. For the best design found by each method, architecture-aware BO reaches a realized aerodynamic efficiency within $1\%$ of the coupled BO result, while reducing the cost by about $50\%$. The best architecture-aware design also improves the shape-tracking error and actuation work with respect to both reference MDO architectures, and remains within the stress and buckling admissibility limits.

These results indicate that architecture-aware BO provides a practical route for optimizing morphing-airfoil systems in which the design value of a target shape can only be assessed after structural realization. The method concentrates expensive coupled evaluations where the realized aerodynamic response is needed, while using sequential-type evaluations to explore the aero-structural design space more efficiently. This is particularly relevant for compliant morphing concepts, where aerodynamic performance, shape recovery, actuation effort, and structural feasibility are strongly coupled. The proposed formulation therefore offers a computationally efficient way to preserve the physical interpretation of coupled design optimization without requiring every candidate to be evaluated through the full coupled chain.

## Acknowledgments

This work is partially supported by the Brahmal Vasudevan Institute for Sustainable Aviation of Imperial College London.

## 6. Contact Author Email Address

l.mainini@imperial.ac.uk

## 7. Copyright Statement

The authors confirm that they hold copyright on all of the original material included in this paper. The authors confirm that they give permission for the publication and distribution of this paper as part of the ICAS proceedings or as individual off-prints from the proceedings.

## References

[1] D. Li, S. Zhao, A. Da Ronch, J. Xiang, J. Drofelnik, Y. Li, L. Zhang, Y. Wu, M. Kintscher, and H. P. Monner. A review of modelling and analysis of morphing wings. *Progress in Aerospace Sciences*, 100:46–62, 2018.

[2] International Energy Agency. Aviation. Available at `https://www.iea.org/energy-system/transport/aviation`, (Accessed: 10/08/2025).

[3] International Air Transport Association (IATA). Our commitment to fly net zero. Available at `https://www.iata.org/en/programs/sustainability/flynetzero/`, (Accessed: 10/08/2025).

[4] R. D. Vocke III, C. S. Kothera, B. K.S. Woods, and N. M. Wereley. Development and testing of a span-extending morphing wing. *Journal of Intelligent Material Systems and Structures*, 22(9):879–890, 2011.

[5] J. Lee, S. Kim, S. Jung, H. Lee, and Y. Kim. Linear parameter-varying control of variable span-sweep morphing aircraft. In *AIAA Scitech 2019 forum*, page 0106, 2019.

[6] R. Vos, Z. Gürdal, and M. Abdalla. Mechanism for warp-controlled twist of a morphing wing. *Journal of Aircraft*, 47(2):450–457, 2010.

[7] T. Yokozeki, A. Sugiura, and Y. Hirano. Development and wind tunnel test of variable camber morphing wing. In *22nd AIAA/ASME/AHS adaptive structures conference*, page 1261, 2014.

[8] A. Islam, A. Rahman, A. K. Saha, and B. W. Jo. Design, implementation, and test flight of a lightweight camber morphing wing aircraft. *American Institute of Aeronautics and Astronautics*, 2025.

[9] A. S. Dale, J. E. Cooper, and A. Mosquera. Adaptive camber-morphing wing using 0-v honeycomb. *American Institute of Aeronautics and Astronautics*, 2013.

[10] S. Vasista, L. Tong, and K.C. Wong. Realization of morphing wings: a multidisciplinary challenge. *Journal of aircraft*, 49(1):11–28, 2012.

[11] J. Sun, Q. Guan, Y. Liu, and J. Leng. Morphing aircraft based on smart materials and structures: A state-of-the-art review. *Journal of Intelligent material systems and structures*, 27(17):2289–2312, 2016.

[12] M Verrastro and I Dimino. Chapter 21 - morphing devices: Safety, reliability, and certification prospects. In A. Concilio, I. Dimino, L. Lecce, and R. Pecora, editors, *Morphing Wing Technologies*, pages 647–682. Butterworth-Heinemann, 2018.

[13] A.Y.N. Sofla, S.A. Meguid, K.T. Tan, and W.K. Yeo. Shape morphing of aircraft wing: Status and challenges. *Materials & Design*, 31(3):1284–1292, 2010.

[14] V. A. Alulema, E. A. Valencia, D. Pillajo, M. Jacome, J. Lopez, and B. Ayala. Degree of deformation and power consumption of compliant and rigid-linked mechanisms for variable-camber morphing wing uavs. *American Institute of Aeronautics and Astronautics*, 2020.

[15] J. J. Joo, C. R. Marks, L. Zientarski, and A. Culler. Variable camber compliant wing - design. *American Institute of Aeronautics and Astronautics*, 2015.

[16] N. M. Alexandrov and M. Yousuff Hussaini. *Multidisciplinary design optimization: State of the art*. SIAM, 1997.

[17] J. Sobieszczanski-Sobieski. Multidisciplinary design optimisation (mdo) methods: Their synergy with computer technology in the design process. *The Aeronautical Journal*, 103(1026):373–382, 1999.

[18] J. R. R. A. Martins and A. B. Lambe. Multidisciplinary design optimization: a survey of architectures. *AIAA journal*, 51(9):2049–2075, 2013.

[19] S. De Gaspari and A. Ricci. A two-level approach for the optimal design of morphing wings based on compliant structures. *Journal of Intelligent Material Systems and Structures*, 22, 2011.

[20] S. De Gaspari and A. Ricci. Design, manufacturing and wind tunnel validation of a morphing compliant wing. *Journal of Aircraft*, 55, 2018.

[21] J. Vale, A. Leite, F. Lau, and A. Suleman. Aero-structural optimization and performance evaluation of a morphing wing with variable span and camber. *Journal of Intelligent Material Systems and Structures*, 2011.

[22] P. Gamboa, J. Vale, F. J. P. Lau, and A. Suleman. Optimization of a morphing wing based on coupled aerodynamic and structural constraints. *AIAA Journal*, 47(9), 2009.

[23] F. Dexl, A. Hauffe, and K. Wolf. Multidisciplinary multi-objective design optimization of an active morphing wing section. *Structural and Multidisciplinary Optimization*, 62:2423–2440, 2020.

[24] J. M. Weaver-Rosen, P. B. C. Leal, D. J. Hartl, and R. J. Malak Jr. Parametric optimization for morphing structures design: application to morphing wings adapting to changing flight conditions. *Structural and Multidisciplinary Optimization*, 2020.

[25] B. M. Kulfan. Recent extensions and applications of the 'cst'universal parametric geometry representation method. *The Aeronautical Journal*, 114(1153):157–176, 2010.

[26] M. Drela. Xfoil: An analysis and design system for low reynolds number airfoils. In *Low Reynolds number aerodynamics: proceedings of the conference notre dame, Indiana, USA, 5–7 June 1989*, pages 1–12. Springer, 1989.

[27] P. I. Frazier. A tutorial on bayesian optimization. *arXiv preprint arXiv:1807.02811*, 2018.

[28] J. Snoek, H. Larochelle, and R. P. Adams. Practical bayesian optimization of machine learning algorithms. *Advances in neural information processing systems*, 25, 2012.

[29] C. Williams and C. Rasmussen. Gaussian processes for regression. *Advances in neural information processing systems*, 8, 1995.

[30] E. Schulz, M. Speekenbrink, and A. Krause. A tutorial on gaussian process regression: Modelling, exploring, and exploiting functions. *Journal of mathematical psychology*, 85:1–16, 2018.

[31] D. R. Jones, M. Schonlau, and W. J. Welch. Efficient global optimization of expensive black-box functions. *Journal of Global optimization*, 13(4):455–492, 1998.